AIAA 81-0094R

General Mapping Procedure for Variable Area Duct Acoustics

James W. White*
The University of Tennessee, Knoxville, Tenn.

A general mapping procedure is described and applied to the study of noise propagation in variable area ducts. The mapping provides a boundary fitted coordinate system which is ideal for the finite-difference solution of acoustic fields with irregular boundaries, without the burden of large matrices required by finite element methods. The procedure is first described in general and then applied to a particular two-dimensional geometry under current experimental investigation. This method should be ideally suited to the study of high-frequency noise propagation in variable area ducts and in cases where the far field is included in the calculation procedure. Moreover, the current approach can be extended directly to three dimensions, resulting in numerical calculation over a rectangular parallelepiped in the transformed plane.

Nomenclature

C_0^*	= ambient speed of sound, m/s
f^*	= frequency, Hz
i	= grid location in ξ direction, also $=\sqrt{-1}$
j	= grid increment in η direction
J	= Jacobian, see Eq. (3)
k	= time level
H^*	= characteristic duct dimension in transverse direction, m
L^*	= duct length, m
n	= normal direction
P	= dimensionless acoustic pressure, $=P^*/(\rho^* C_0^{*2})$, also grid control function
Q	= grid control function
t	= dimensionless time, $=t^*f^*$
t^*	= time, s
u	= dimensionless acoustic velocity in x direction, $=u^*/C_0^*$
u^*	= acoustic velocity in x direction, m/s
v	= dimensionless acoustic velocity in transverse direction, $=v^*/C_0^*$
v^*	= acoustic velocity in transverse direction, m/s
X	= dimensionless axial coordinate, $=X^*/H^*$
X^*	= axial coordinate
Y	= dimensionless transverse coordinate, $=Y^*/H^*$
Y^*	= transverse coordinate, m
α,β,γ	= see Eq. (5)
$\Delta\xi,\Delta\eta$	= increments in transformed plane
∇	= gradient operator
$\delta_{\xi\xi},\delta_{\eta\eta}$	= second-order finite-difference operators
ζ	= specific acoustic impedance
ξ,η	= coordinates in transformed plane
ρ^*	= ambient fluid density, kg/m^3
ω	= dimensionless frequency, $=H^*f^*/C_0^*$

Introduction

DURING the past ten years, the study of noise propagation in ducts has received considerable attention, due to the introduction of strict aircraft noise regulations. The analytical approaches developed divide into several areas. Steady-state finite-difference theory[1-4] assumes the acoustic properties are simple harmonic functions of time, resulting in governing mathematics which are independent of time. However, these steady-state equations tend to be difficult to solve numerically. Steady-state finite element theory[5-18] is quite useful in the study of acoustical systems with boundaries that possess sharp curvature or slope discontinuity. However, in situations where many elements are required, large matrices must be used, which can burden even the largest of computers. Special numerical transformation methods[19-22] have appeared but tend to be specialized to rather particular situations. During the past few years, transient numerical theory has been demonstrated by Baumeister[23-25] as an alternative to the finite element approach. The transient method approach requires no large matrices and is relatively simple to code. Of course, this approach in finite-difference form does have difficulty in accurately satisfying boundary conditions on irregular surface boundaries.

An accurate numerical description of boundary location and boundary condition is very important since the overall solution of noise propagation is influenced strongly by the acoustic boundary conditions. When an irregular boundary must be dealt with usually one of two approaches is taken. The boundary can be located approximately with a uniform grid or it can be located exactly by use of a variable spatial grid. Neither of these approaches is desired. The first introduces error into the boundary condition. The second approach results in less accurate finite-difference approximations and tends to require tailoring to a particular geometry and so is more cumbersome to use. In order to most accurately represent boundary conditions numerically, the boundary should be coincident with a coordinate line. The generation of a boundary fitted coordinate system is then quite desirable.

A general approach to the development of such a coordinate system is to allow the curvilinear coordinates to be solutions of an elliptic partial-differential equation (PDE) system in the physical plane with Dirichlet conditions on all boundaries. With this method, one coordinate is constant along each of the boundaries. Grid points may be concentrated as desired on the boundary in the physical plane, and the procedure is not restricted to two dimensions. The resulting coordinate system is, in general, not orthogonal, but this presents no problem.

This approach has been applied to two-dimensional simply connected regions by Winslow,[26] Barfield,[27] Chu,[28] Amsden and Hirt,[29] and Godunov and Prokopov.[30] Winslow[26] and Chu[28] took the transformed coordinates to be solutions of a Laplace equation in the physical plane which produces the physical coordinates as solutions of a quasilinear elliptic system in the transformed plane. Thompson et al.[31,32] followed this approach and developed a method for the construction of a body-fitted coordinate system over a multiply connected region, with application to aerodynamic

Presented as Paper 81-0094 at the AIAA 19th Aerospace Sciences Meeting, St. Louis, Mo., Jan. 12-15, 1981; submitted March 11, 1981; revision received Nov. 13, 1981.

*Associate Professor, Department of Mechanical and Aerospace Engineering.

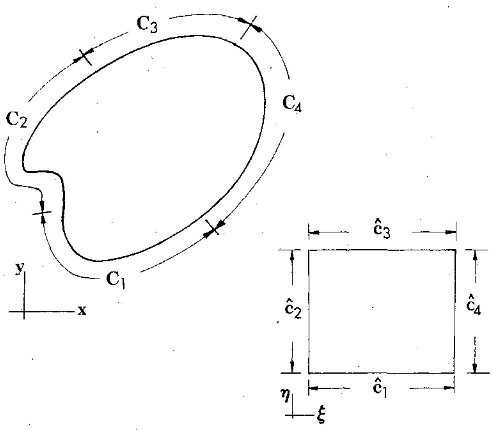

Fig. 1 The physical and transformed planes.

flows. Solution of the mapping equations by Thompson et al.[31,32] is achieved by successive over-relaxation (SOR). The speed of convergence and, indeed, convergence itself is dependent on the initial conditions of the physical coordinates.

The purpose of this paper is to present the development of a general mapping procedure applicable to variable area duct acoustics studies. The mapping provides an accurate resolution of the flow boundaries and provides a convenient computational plane for solution of the governing physical equations using finite differences. Since many of the details of the derivation of the PDE mapping system are included in Ref. 32, only an outline will be included here. The solution method used for the mapping is quite different than any obtained earlier, however, and is described here in detail. Computed results are included for the mapping of a variable area two-dimensional duct. The transformed zero flow acoustic equations and boundary conditions are also derived for the same geometry. These equations then are solved numerically, and the results are compared with experimental values.

Mapping Procedure

In order to illustrate the mapping procedure, consider the general two-dimensional domain shown on Fig. 1. The boundary is continuous but may possess steep curvature and/or slope discontinuity. We define a mapping that transforms the domain in the physical (X-Y) plane into a rectangle in the (ξ-η) plane. Grid points may be placed arbitrarily along the boundary in the physical plane; the mapping allows these points to be located equally spaced along corresponding segments in the transformed plane. This feature of the mapping then allows points to be condensed in regions of the physical plane where the governing physical equations are expected to produce steep gradients, while computation is performed over a uniform grid where central difference numerical approximations may be used. The physical coordinates of the interior points in the transformed plane are unknown and must be solved for by use of the mapping equations. Let the mapping be defined by the following system of elliptic equations:

$$\nabla^2\xi = P(\xi,\eta) \qquad \nabla^2\eta = Q(\xi,\eta) \tag{1}$$

The functions P and Q are used to control the location of the grid lines and are used frequently in aerodynamics calculations where one of the transformed coordinates may not intersect a flow boundary. The dependent and independent variables in Eqs. (1) are interchanged as follows:

$$f_\xi = f_x X_\xi + f_y Y_\xi \qquad f_\eta = f_x X_\eta + f_y Y_\eta \tag{2}$$

Equations (2) are then solved to give

$$f_x = (f_\xi Y_\eta - f_\eta Y_\xi)/J$$

and

$$f_y = (-f_\xi X_\eta + f_\eta X_\xi)/J \tag{3}$$

where

$$J = X_\xi Y_\eta - X_\eta Y_\xi$$

Thus, we have

$$\xi_x = Y_\eta / J \qquad \xi_y = -X_\eta / J \tag{4}$$

and so on. The Laplacian operators then appear as

$$J^3\nabla^2\xi = X_\eta[\alpha Y_{\xi\xi} - 2\beta Y_{\xi\eta} + \gamma Y_{\eta\eta}] - Y_\eta[\alpha X_{\xi\xi} - 2\beta X_{\xi\eta} + \gamma X_{\eta\eta}]$$

$$J^3\nabla^2\eta = -X_\xi[\alpha Y_{\xi\xi} - 2\beta Y_{\xi\eta} + \gamma Y_{\eta\eta}] + Y_\xi[\alpha X_{\xi\xi} - 2\beta X_{\xi\eta} + \gamma X_{\eta\eta}] \tag{5}$$

where

$$\alpha = X_\eta^2 + Y_\eta^2 \qquad \beta = X_\xi X_\eta + Y_\xi Y_\eta \qquad \gamma = X_\xi^2 + Y_\xi^2$$

Using Eqs. (5) and (1) and solving for the second-order grouped terms in Eqs. (5), there results

$$\alpha X_{\xi\xi} - 2\beta X_{\xi\eta} + \gamma X_{\eta\eta} + J^2[X_\xi P + X_\eta Q] = 0 \tag{6a}$$

$$\alpha Y_{\xi\xi} - 2\beta Y_{\xi\eta} + \gamma Y_{\eta\eta} + J^2[Y_\xi P + Y_\eta Q] = 0 \tag{6b}$$

The coupled quasilinear elliptic system Eqs. (6) is then solved in the transformed plane for the physical coordinates X and Y.

The solution of Eqs. (6) in the current work departs markedly from the SOR procedure reported by Thompson et al.[31,32] The coefficients of the second-order terms are nonlinear which makes the numerical solution by SOR highly dependent on the initial conditions used. In the current work, a different approach is taken. In order to minimize the influence of the initial conditions on the stability and convergence of the solution, a damping term is added to each of the PDE's in Eqs. (6), resulting in

$$X_t = \alpha X_{\xi\xi} - 2\beta X_{\xi\eta} + \gamma X_{\eta\eta} + J^2[X_\xi P + X_\eta Q] \tag{7a}$$

$$Y_t = \alpha Y_{\xi\xi} - 2\beta Y_{\xi\eta} + \gamma Y_{\eta\eta} + J^2[Y_\xi P + Y_\eta Q] \tag{7b}$$

The mapping equations given by Eqs. (6) express geometric relationships between the coordinate terms and, of course, involve no real-time dependence. The motivation here is that the time derivative terms will serve to smooth out and dampen the simultaneous solution of the two equations. The "steady-state" solution of Eqs. (7) is then viewed as the asymptotic transient solution as time approaches infinity.

In the development that follows, the grid control terms P and Q are neglected. Control terms are useful primarily in the analysis of multiply connected domains where some contour lines do not touch the boundary. For mapping of simply connected domains, grid points concentrated on the physical boundary can provide the same effect as the grid control terms.

The numerical solution of Eqs. (7) is obtained by an alternating direction implicit method. The method exhibits spatial factoring and reduces to a series of tridiagonal matrix inversions in progressing from one time level to the next.

Factored schemes have developed significantly since their introduction[33] and are currently used for complex calculations such as the Navier-Stokes equation.[34]

When Eqs. (7) are expressed in finite-difference form using Crank-Nicholson averaging, there results

$$\left(1-\alpha\frac{\Delta t}{2}\delta_{\xi\xi}\right)\left(1-\frac{\gamma\Delta t}{2}\delta_{\eta\eta}\right)(X^{k+1}-X^k)$$

$$=[\alpha X^k_{\xi\xi}-2\beta X^k_{\xi\eta}+\gamma X^k_{\eta\eta}]\Delta t-\beta[X^k_{\xi\eta}-X^{k-1}_{\xi\eta}]\Delta t \tag{8a}$$

$$\left(1-\alpha\frac{\Delta t}{2}\delta_{\xi\xi}\right)\left(1-\gamma\frac{\Delta t}{2}\delta_{\eta\eta}\right)(Y^{k+1}-Y^k)$$

$$=[\alpha Y^k_{\xi\xi}-2\beta Y^k_{\xi\eta}+\gamma Y^k_{\eta\eta}]\Delta t-\beta[Y^k_{\xi\eta}-Y^{k-1}_{\xi\eta}]\Delta t \tag{8b}$$

In Eqs. (8), the nonlinear coefficients (α,β,γ) are treated explicitly as the solution progresses from one time level (k) to the next $(k+1)$. The finite-difference Eqs. (8) are in the form

$$(1-L_1)(1-L_2)\Delta X^k=\phi_1 \tag{9a}$$

$$(1-L_1)(1-L_2)\Delta Y^k=\phi_2 \tag{9b}$$

where

$$\Delta X^k=X^{k+1}-X^k \qquad \Delta Y^k=Y^{k+1}-Y^k$$

L_1 is the linear difference operator in ξ direction and L_2 the linear difference operator in η direction. The factored solution is achieved by first solving values of X and Y at an intermediate time (denoted by an asterisk) from

$$(1-L_1)\Delta X^*=\phi_1 \tag{10a}$$

$$(1-L_1)\Delta Y^*=\phi_2 \tag{10b}$$

Equations (10a) and (10b) each represent a system of one-dimensional equations in the ξ direction. Each equation requires a tridiagonal matrix inverse. The final values at the new time $(k+1)$ are then obtained from

$$(1-L_2)\Delta X^k=\Delta X^* \tag{11a}$$

$$(1-L_2)\Delta Y^k=\Delta Y^* \tag{11b}$$

Equations (10) and (11) are equivalent to Eqs. (9). This can be seen by operating on Eq. (11a) with $(1-L_1)$ and adding the result to Eq. (10a). The result is Eq. (9a). A similar procedure shows that Eqs. (10b) and (11b) are equivalent to Eq. (9b). As an example consider a two-dimensional duct with a variable area. The top surface (see Fig. 2) is given by a fourth-degree polynomial which appears as

$$\hat{Y}/h=16(X/L)^2-32(X/L)^3+16(X/L)^4 \tag{12}$$

and produces a 50% decrease in flow area at the duct midlength. The initial values of X and Y were assumed to vary linearly in the transformed plane. Equations (8) were integrated in time and convergence was achieved in twenty time steps for an 11×11 grid. The resulting grid distribution is plotted on Fig. 3. For this particular geometry, the constant ξ lines remain vertical, because the inlet and exit boundaries are vertical. The vertical distance between constant η lines is not constant and reflects the effect of the curved top wall on the overall grid distribution. The acoustic properties of this particular variable area duct currently are under study at NASA Lewis Research Center. In the next section, the linearized acoustic equations are transformed and solved numerically; results are compared with experiment.

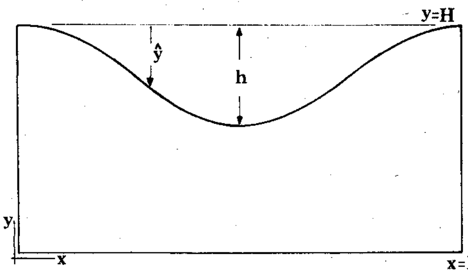

Fig. 2 A variable area two-dimensional duct.

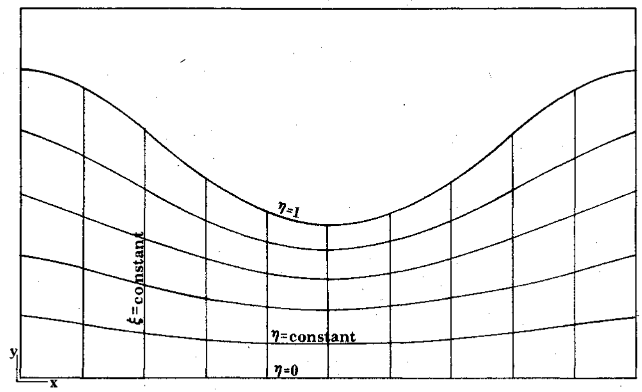

Fig. 3 Solution of the mapping for a variable area duct.

Transformation of the Acoustic Equations

For the case of two-dimensional zero mean flow, the linearized acoustic equations of continuity and momentum appear, respectively, as

$$\omega P_t=-u_x-v_y \qquad \omega u_t=-P_x \qquad \omega v_t=-P_y \tag{13}$$

where all terms are nondimensional and are defined in the Nomenclature. The component equations of Eqs. (13) can be combined into a single wave equation which appears as

$$\omega^2 P_{tt}=P_{xx}+P_{yy} \tag{14}$$

Boundary conditions for the variable area two-dimensional duct shown in Fig. 2 follow.

Inlet $(X=0)$:

$$P=\exp(i2\pi t) \tag{15}$$

This is the noise source that drives the acoustic flow.

Bottom $(Y=0)$:

$$\frac{\omega}{\zeta}P_t-P_y=0 \tag{16}$$

Here, ζ is the specific acoustic impedance. For cases where $y=0$ corresponds to a line of symmetry or where a hard wall condition $(\zeta\rightarrow\infty)$ is applied, Eq. (16) reduces to

$$P_y=0$$

Exit $(x=L^*/H^*)$:

$$\omega P_t+P_x=0 \tag{17}$$

Equation (17) assures that no plane wave reflection occurs at the duct exit and so approximates the condition of an infinite length constant diameter duct beyond the variable area duct exit.

Top surface:

$$\frac{\omega}{\zeta}P_t+P_n=0 \tag{18}$$

Here, n is the normal in the outer direction to the duct top surface. For the case of a hard wall, the boundary condition given by Eq. (18) reduces to

$$P_n = 0$$

Upon transforming to the (ξ-η) plane, the wave Eq. (14) appears as

$$\omega^2 P_{tt} = \frac{1}{J^2}\left[\alpha P_{\xi\xi} - 2\beta P_{\xi\eta} + \gamma P_{\eta\eta} + \sigma P_\eta + \tau P_\xi\right] \tag{19}$$

where (α,β,γ,J) are defined as before and

$$\sigma = J^2 Q \qquad \tau = J^2 P$$

For this particular case, since no grid control terms were used in the mapping, we have

$$\sigma = \tau = 0$$

The transformed boundary conditions appear as follows.

Inlet ($\xi = 0$):

$$P = \exp(i2\pi t) \tag{15}$$

Bottom ($\eta = 0$):

$$\frac{\omega}{\zeta} P_t - \frac{\sqrt{\gamma}}{J} P_\eta = 0 \tag{20}$$

Exit ($\xi = 1$):

$$\omega P_t + \frac{1}{J}\left[Y_\eta P_\xi - Y_\xi P_\eta\right] = 0 \tag{21}$$

Top surface ($\eta = 1$):

$$\frac{\omega}{\zeta} P_t + \frac{1}{J\sqrt{\gamma}}\left[\gamma P_\eta - \beta P_\xi\right] = 0 \tag{22}$$

The mapping procedure does not introduce nonlinearities into the wave equation or the associated boundary conditions. However, the mapping does bring variable coefficients into the governing mathematics.

The transformed wave equation is then put into second-order time-accurate finite-difference form for an explicit solution and appears as

$$\omega^2 \frac{P^{k+1}_{i,j} - 2P^k_{i,j} + P^{k-1}_{i,j}}{(\Delta t)^2} = \frac{1}{J^2}\left[\alpha P^k_{\xi\xi} - 2\beta P^k_{\xi\eta} + \gamma P^k_{\eta\eta}\right] \tag{23}$$

where

$$P^k_{\xi\xi} = \frac{P^k_{i+1,j} - 2P^k_{i,j} + P^k_{i-1,j}}{(\Delta\xi)^2}$$

$$P^k_{\eta\eta} = \frac{P^k_{i,j+1} - 2P^k_{i,j} + P^k_{i,j-1}}{(\Delta\eta)^2}$$

$$P^k_{\xi\eta} = \frac{1}{4\Delta\xi\Delta\eta}\left[P^k_{i+1,j+1} + P^k_{i-1,j-1} - P^k_{i+1,j-1} - P^k_{i-1,j+1}\right]$$

The system of equations given by Eq. (23) together with the finite-difference form of the boundary conditions Eqs. (15), (20), (21), and (22) were solved on the rectangular transformed domain for the case of a hard wall duct with the geometry shown on Fig. 3. The computational grid used was 11×11 with a dimensionless time increment of 0.002 while the initial condition on the acoustic pressure was that of a quiescent field. It should be noted that since the noise source is complex, the resulting pressure throughout the duct will also be complex. For large values of time, the acoustic

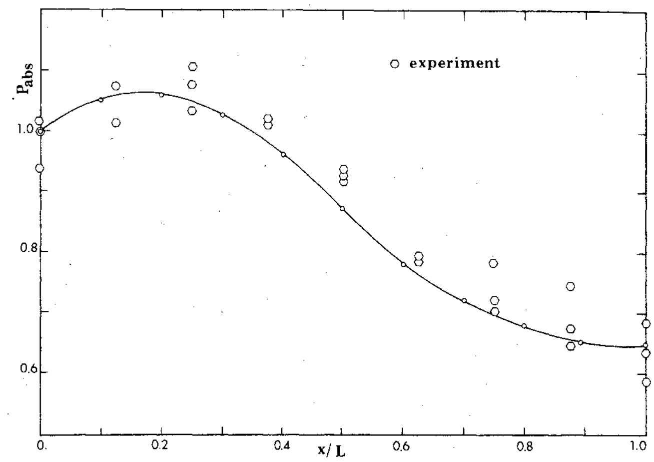

Fig. 4 Comparison of the computed and measured pressure profiles for the variable area duct.

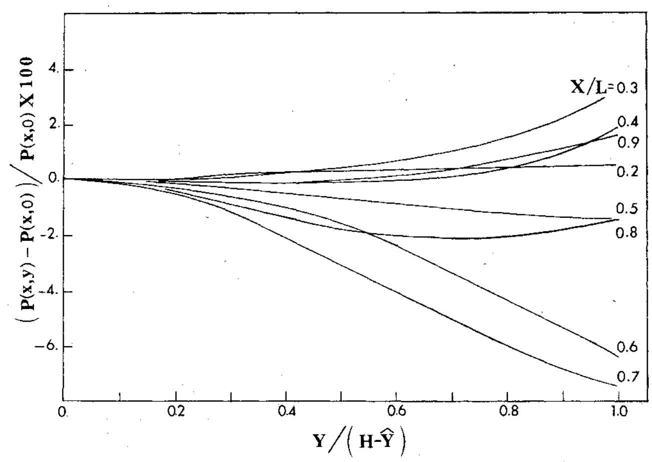

Fig. 5 Computed transverse pressure profiles for the variable area duct.

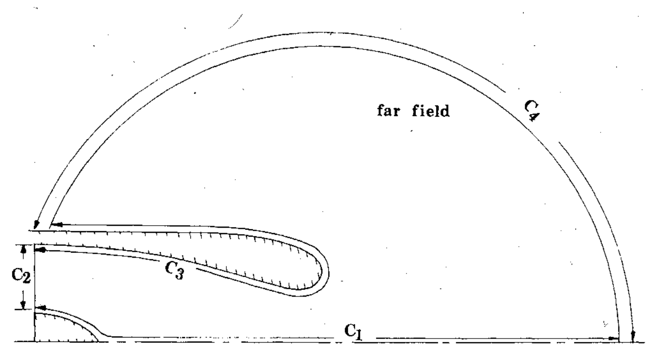

Fig. 6 Inclusion of the far field with a variable area engine inlet.

pressure field takes the form

$$P = \hat{P}(X,Y)\exp(i2\pi t)$$

where

$$\hat{P} = \hat{P}_1(X,Y) + i\hat{P}_2(X,Y)$$

Numerical results of the bottom wall absolute pressure given by

$$P_{\text{abs}} = \left|\frac{P(X,Y=0,t)}{\exp(i2\pi t)}\right|$$

are presented on Fig. 4 after 800 time steps of integration for a dimensionless frequency of 0.172. Computed transverse pressure profiles are shown on Fig. 5. After this much simulated time, the absolute pressure essentially is independent of time, resulting in a periodic steady state. Agreement with the experimental data supplied by NASA Lewis Research Center is seen to be good, although some scatter does exist in the experimental values. Required central processing unit time for the mapping and time dependent solution was about 60 s on an IBM 370/3031 system.

The example illustrates the mapping procedure and the resulting numerical solution of the transformed wave equation and associated boundary conditions. The full power of this mapping method will be increasingly evident in the study of more complicated geometries and in cases where the far field is included in the computation, as shown on Fig. 6. Inclusion of the far field will provide acoustic radiation patterns far from the noise source and will eliminate the necessity of specifying approximate boundary conditions at the duct exit.

Conclusion

A general mapping procedure has been described which is applicable to the study of noise propagation in variable area ducts. The method combines the most desirable characteristics of finite differences and finite elements in that highly accurate boundary resolution is provided without the need for large matrices. These features will be especially important in the study of very high-frequency noise propagation.

In two dimensions, the mapping is more general and less restrictive than a conformal map. Moreover, the mapping described here can be extended directly to three dimensions, resulting in finite-difference calculation over a rectangular parallelepiped in the transformed plane.

Acknowledgments

The work reported here was supported by NASA Lewis Research Center under Contract NAG3-18. The NASA Technical Officer for the grant is Dr. K. J. Baumeister.

References

[1] Alfredson, R. J. "A Note on the Use of the Finite Difference Method for Predicting Steady State Sound Fields," *Acoustica*, Vol. 28, May 1973, pp. 296-301.

[2] Baumeister, K. J. and Rice, E. J., "A Difference Theory for Noise Propagation in an Acoustically Lined Duct with Mean Flow," AIAA *Progress in Astronautics and Aeronautics—Aeroacoustics: Jet and Combustion Noise; Duct Acoustics*, edited by H. T. Nagamatsu, J. V. O'Keefe, and I. R. Schwartz, Vol. 37, New York, 1975, pp. 435-453.

[3] Baumeister, K. J., "Time Dependent Difference Theory for Noise Propagation in Jet Engine Ducts," AIAA Paper 80-0098, Jan. 1980.

[4] Quinn, D. W., "A Finite Difference Method for Computing Sound Propagation in Nonuniform Ducts," AIAA Paper 74-130, Jan. 1974.

[5] Young, C.-I., James and Crocker, M., "Prediction of Transmission Loss in Mufflers by the Finite-Element Method," *Journal of the Acoustic Society of America*, Vol. 57, Jan. 1975.

[6] Kagawa, Y. and Omote, T., "Finite-Element Simulation of Acoustic Filters of Arbitrary Profile with Circular Cross Section," *Journal of the Acoustic Society of America*, Vol. 60, Nov. 1976.

[7] Craggs, A., "A Finite Element Model for Rigid Porous Absorbing Materials," *Journal of Sound and Vibration*, Vol. 61, No. 1, 1978, pp. 101-111.

[8] Craggs, A., "Coupling of Finite Element Acoustic Absorption Models," *Journal of Sound and Vibration,* "Vol. 66, No. 4, 1979, pp. 605-613.

[9] Tag, I. A. and Lumsdaine, E., "A Finite Element Approach to the Problem of Noise Propagation and Attenuation in Industrial Duct," presented at the ASME Annual Meeting, San Francisco, Calif., Dec. 1978.

[10] Tag, I. A. and Akin, J. E., "Finite Element Solution of Sound Propagation in a Variable Area Duct," AIAA Paper 79-0663, March 1979.

[11] Tag, I. A. and Lumsdaine, E., "An Efficient Finite Element Technique for Sound Propagation in Axisymmetric Hard Wall Ducts Carrying High Subsonic Mach Number Flows," AIAA Paper 78-1154, July 1978.

[12] Sigman, R. K., Majjigi, R. K., and Zinn, B. T., "Determination of Turbofan Inlet Acoustics Using Finite Elements," *AIAA Journal*, Vol. 16, Nov. 1978, pp. 1139-1145.

[13] Majjigi, R. K., "Application of Finite Element Techniques in Predicting the Acoustic Properties of Turbofan Inlets," Ph.D. Thesis, Georgia Institute of Technology, Atlanta, Ga., 1979.

[14] Majjigi, R. K., Sigman, R. K., and Zinn, B. T., "Wave Propagation in Ducts Using the Finite Element Method," AIAA Paper 79-0659, March 1979.

[15] Astley, R. J. and Eversman, W., "A Finite Element Method for Transmission in Non-Uniform Ducts Without Flow: Comparison with the Method of Weighted Residuals," *Journal of Sound and Vibration*, Vol. 57, April 1978, pp. 367-388.

[16] Eversman, W., Astley, R. J., and Thanh, V. P., "Transmission in Non-Uniform Ducts—A Comparative Evaluation of Finite Element and Weighted Residuals Computational Schemes," AIAA Paper 77-1299, Oct. 1977.

[17] Astley, R. J. and Eversman, W., "The Application of Finite Element Techniques to Acoustic Transmission in Lined Ducts with Flow," AIAA Paper 79-0660, March 1979.

[18] Thanh, V. P., "Computational Methods for Sound Transmission in Non-Uniform Waveguides," Ph.D. Thesis, University of Canterbury, June 1979.

[19] Baumeister, K. J., "Analysis of Sound Propagation in Ducts Using the Wave Envelope Concept," NASA TN D-7719, 1974.

[20] Baumeister, K. J., "Wave Envelope Analysis of Sound Propagation in Ducts with Variable Axial Impedance," AIAA *Progress in Astronautics and Aeronautics—Aeroacoustics: Duct Acoustics, Fan Noise and Control Rotor Noise,* edited by I. R. Schwartz, H. T. Nagamatsu, and W. Strahle, Vol. 44, New York, 1976, pp. 451-474.

[21] Baumeister, K. J., "Numerical Spatial Marching Techniques for Estimating Duct Attenuation and Source Pressure Profiles," 95th Meeting of the Acoustical Society of America, Providence, R. I., May 1978; also, NASA TM-78857, 1978.

[22] Baumeister, K. J., "Numerical Spatial Marching Techniques in Duct Acoustics," *Journal of the Acoustical Society of America,* Vol. 65, Feb. 1979, pp. 297-306.

[23] Baumeister, K, J., "Time Dependent Difference Theory for Noise Propagation in Jet Engine Ducts," AIAA Paper 80-0098, Jan. 1980.

[24] Baumeister, K. J., "A Time Dependent Difference Theory for Sound Propagation in Ducts with Flow," 98th Meeting of the Acoustical Society of America, Salt Lake City, Nov. 1979; also, NASA TM-79302, 1979.

[25] Baumeister, K. J., "Time Dependent Difference Theory for Sound Propagation in Axisymmetric Ducts with Flow," AIAA Paper 80-1017, June 1980.

[26] Winslow, A. J., "Numerical Solution of the Quasi-Linear Poisson Equation in a Non-Uniform Triangular Mesh," *Journal of Computational Physics,* Vol. 2, 1966, p. 149.

[27] Barfield, W. D., "An Optimal Mesh Generator for Lagrangian Hydrodynamic Calculations in Two Space Dimensions," *Journal of Computational Physics,* Vol. 6, 1970, p. 417.

[28] Chu, W. H., "Development of a General Finite Difference Approximation for a General Domain, Part I: Machine Transformation," *Journal of Computational Physics,* Vol. 8, 1971, p. 392.

[29] Amsden, A. A. and Hirt, C. W., "A Simple Scheme for Generating General Curvilinear Grids," *Journal of Computational Physics,* Vol. 11, 1973, p. 348.

[30] Godunov, S. K. and Prokopov, G. P., "The Use of Moving Meshes in Gas Dynamics Computations," *USSR Computational Mathematics and Mathematical Physics,* Vol. 12, 1972, p. 182.

[31] Thompson, J. F., Thames, F. C., and Mastin, C. W., "Automatic Numerical Generation of Body-Fitted Curvilinear Coordinate System for Field Containing Any Number of Arbitrary Two-Dimensional Bodies," *Journal of Computational Physics,* Vol. 15, July 1974, p. 299.

[32] Thompson, J. F., Thames, F. C., and Mastin, C. W., "Boundary-Fitted Curvilinear Coordinate System for Solution of Partial Differential Equations on Fields Containing Any Number of Arbitrary Two-Dimensional Bodies," NASA CR-2729, July 1977.

[33] Douglas, J., "On the Numerical Integration of $u_{xx}+u_{yy}=u_t$ by Implicit Methods," *Journal of the Society of Industrial Applied Mathematics,* Vol. 3, 1955, pp. 42-65.

[34] Briley, W. R. and McDonald, H., "Solution of the Multi-Dimensional Compressible Navier-Stokes Equations by a Generalized Implicit Method," *Journal of Computational Physics,* Vol. 24, 1977, pp. 372-397.